Hydrogen Storage Evolution on Intermetallic LaMg$_2$Ni$_5$Al$_4$

Hassen Jaafar*‡ (iD), Chiheb Slama** (iD), Ines Sahli* (iD), Arij Dhiab*** (iD),

Marwa Ayari* (iD), Mohieddine Abdellaoui* (iD)

* Institut National de Recherche et d'Analyse Physico-chimique, BiotechPole Sidi Thabet, 2020 Ariana, Tunisia

** Ecole Supérieure d'Ingénieurs de Medjez El Bab, Université de Jendouba, 9070, Tunisia

*** Institut National des Sciences Appliquées et de Technologie, Université de Carthage, 1080 Tunis, Tunisia

(hassen.jaafar@inrap.rnrt.tn, chihebslama@yahoo.fr, sahli.ines86@yahoo.fr, dhiab.arij@gmail.com, marwaayari28@yahoo.fr, mohieddine.abdellaoui@gmail.com)

‡ Corresponding Author; Hassen Jaafar, Institut National de Recherche et d'Analyse Physico-chimique,

BiotechPole Sidi Thabet, 2020 Ariana, Tunisia, Tel: +216 26 593 543, hassen.jaafar@inrap.rnrt.tn,

Abstract- Research on hydrogen storage alloys is offering actually a wide range of chemisorption-materials that can store or release safely interesting amount of hydrogen regarding classic pressurized or cryo-liquid container needing expensive and permanent maintenance procedure. In this context, rigorous hydrogenation experiment was elaborated on new AB$_3$ compound LaMg$_2$Ni$_5$Al$_4$ recently investigated as quaternary intermetallic material. X-ray diffraction analysis shows that two different pathways could be used from elementary metals or binary precursors to fulfil the desired crystal phase. Careful screening of the AB$_3$ alloy thermal stability was carried out before hydrogenation. Differential thermal analysis DTA demonstrates that this compound can support heating flow up 800 °C without any degradation. Straight solid-gas hydrogenation process was controlled and acquired following meticulously the pressure. It was demonstrated that hydrogen sorption is following a first-order exponential Avrami model. Interestingly, the kinetic study illustrates that lower activation energy (a gap of 90 kJ.mol^{-1}) is observed comparing the intermetallic from binary precursor. Results show also that this compound is prominent candidate serving stabilized solid-Hydrogen as bulk reservoir and hydrogen absorption measurement endorsed that bulk intermetallic hydride is achieved.

Keywords Metals and alloys, Hydrogen storage, Thermal analysis, Intermetallic compounds.

1. Introduction

To limit greenhouse-gas emissions and depletion of fossil carbon reserves, implementation of technologies involving renewable energies and their conversion is an absolute priority for the inevitable forthcoming ecological transition [1]. In first place: hydrogen, which is clean efficient fuel, its combustion produces only water H$_2$O (low environment impact) and having reliable storage output [2,3]. Renewable hydrogen using green technology could make worldwide fossil-free faster than expected. Hydrogen can be stored as compressed gas, cryogenic liquid (low temperature) or solid form. The storage under high pressure or cryogenic liquid does not allow accessing higher densities regarding solid hydrogen in intermetallic hydrides [4,5]. Utilization of

metal-hydrides is currently considered as key point for future hydrogen economy regarding several criterions like safety, compaction, and reversibility [6,7]. A very interesting paper was published over the past decade by Chen et al. [8] reporting on hydrogenation properties of related compounds like LaCaMgNi$_9$ and others high entropy alloys like LaCaMgNi$_6$Al$_3$. Chen et al. [8] conducted extensive hydrogen sorption isotherms and demonstrated that using Aluminium (Al atomic radius is lower than Ni) to substitute Nickel reduces the unit cell expansion ($\Delta V/V$) during solid-gas hydrogen reaction. They noticed furthermore that Al/Ni substitution induces lower hydrogen equilibrium pressure [8]. These prominent hints are considered as good parameters when industrial researchers are looking for long life cycling product during reversible hydriding process: because

controlling cell expansion would substantially decrease compounds cracking. Besides, lowering H_2 pressure is valuable point towards improved safe handling or embedded hydrogen storage in mobile devices [9,10]. Another detailed electrochemistry coupled X-ray diffraction study was carried out by Liao et al. [11] on rich Lanthanum AB_3 compounds $La_2Mg(Ni_{1-x}M_x)_9$ with M = Fe, Co, Al, Mn, or Cu. They confirmed that Nickel partial substitution using other transition metals will affect hydrogen plateau pressure and cell expansion of relative hydrides depending on atomic radius of M element. Several analytical kinetics models were developed during the past decades to determine hydrogen reaction rate and the corresponding activation energy; and the controlling-rate mechanisms which involve diffusion phenomena and growth following nucleation [12-14]. Generally, these two parameters are acquired by fitting the kinetics curves using Avrami equation and the slope from Arrhenius plot:

Exponential interpolation of first-order Avrami Equation: $C_t = C_{max} \exp(-k \cdot t)$

where k is the hydrogenation reaction speed conforming to Arrhenius Law

The main objective of this article is to undertake comparative kinetic study for two intermetallic samples synthesized by different pathways approach. Experimental measurements of hydrogen absorption are examined and inspected for a prospective convergent correlation toward this first-order exponential Avrami model.

With the research outbreaks during the last years about intermetallics hydrogen uptake [15-22], more significant or comprehensive studies were developed showing the importance of metal substitutions and their influence on thermodynamic parameters [23-29]. The present paper is reporting on the hydrogen storage evolution of an AB_3 quaternary alloy $LaMg_2Ni_5Al_4$ and its Differential thermal analysis DTA. The original aspect of this work is to show that the type of synthesis reaction and the starting precursors used to elaborate the same target intermetallic phase can play an important role in moderating the corresponding activation energy. This suggests further implications of several intrinsic matrix considerations like difference in: structure defects, material density, ratio of amorphous to crystal state, active or specific surface, particles size and existence of joint grain.

2. Experimental materials and methods

$LaMg_2Ni_5Al_4$ intermetallic alloy was elaborated regarding previous published work [30] in the laboratory from elementary pure metals introduced inside stainless steel jar with 5 stainless-steel balls in argon filled glovebox. The mechanical alloying MA experiment was performed during 20 hours at ambient temperature with Fritsch "Pulverisette P7" planetary ball mill. Disc and jar rotation speeds were respectively 550 and 1100 rpm. These mechanical alloying procedures correspond to an injected shock power, kinetic shock energy and a shock frequency of respectively 12 W/g, 0.105 J/hit and 114 Hz. Differential Thermal Analysis DTA was done to screen any transformation and to check the stability of the compound for medium or high temperature

before starting the hydrogenation reaction. This analysis experiment was carried out with an inert atmosphere using an instrument type PerkinElmer. Determination of the real solid density of $LaMg_2Ni_5Al_4$ intermetallic alloy was acquired using Micromeritics AccuPyc II 1340 Helium Pycnometer. The sample analysis gives $\rho = 5.58$ g/cm^3.

For hydrogen storage experiment using Sieverts method (Figure 1), 0.415 g of intermetallic AB_3 alloy achieved from pure elements or from binary precursors was introduced in hydrogenation capsule set to vacuum overnight at temperature of 280 °C. After that the capsule capillary was first isolated, hydrogen pressure of 10 bars was loaded in the system and then released into the sample. The hydrogenation test bench is consisted of a setup Swagelok type materials connected with several input/output valves, sample holder, pressure input regulators and pressure sensors. Connectors and bench devices are leakage tested using snoops under pressurized condition before starting any acquisition. All pressure devices are calibrated from the provider and having their datasheet of linear voltage to pressure response. The pressure conversion into hydrogen capacity is based on the Sievert Method relating the partial pressure according to the perfect gas Law in the local domain of temperature and pressure measurements. The pressure evolution was followed using ADI gas sensor linked to DITEL Alpha-C remote display. This pressure display was controlled using an acquisition card connected to HP BenchLink Data Logger and then hydrogen kinetics correlation was done using WaveMetrics IgorPro 4.0.8. software.
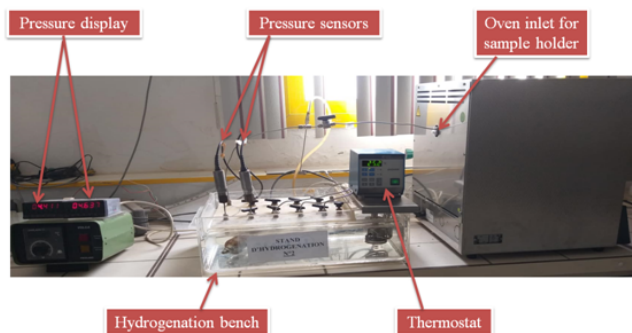

Fig. 1. Experimental device for solid-gas hydrogen evolution

3. Results and Discussions

This AB_3 intermetallic lanthanide has been directly synthesized using the ball milling technique without further treatment and its full structural and microstructure characterization was also extensively studied.

Starting from elementary metals (La:Mg:Ni:Al in atomic proportion 1:2:5:4), it was shown that a resulting crystalline material is obtained and the structural analysis (Figure 2 and Table 1) confirms that it constitutes almost a single AB_3 phase product [30]. It is also demonstrated in this section according to Figure 3 and Table 2 that AB_3 intermetallic lanthanide can be achieved as well starting from binary compounds $LaNi_5$ and Mg:Al(33:66). Furthermore, it is found that same composition phases are obtained regarding

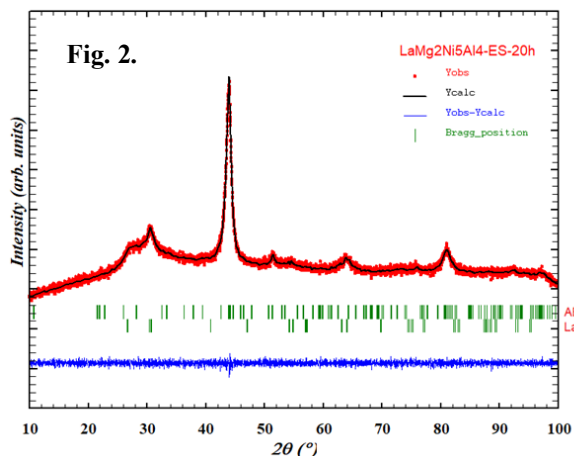the previous prepared sample from elementary metals with practically equivalent weight proportion.

Fig. 2. Rietveld refinement of LaMg$_2$Ni$_5$Al$_4$-ES-20h (from elementary metals).
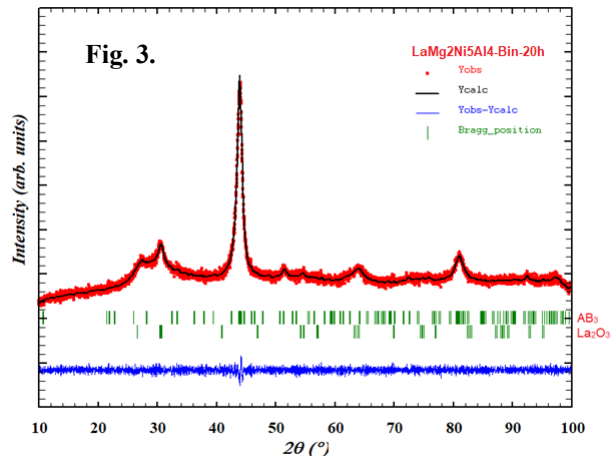
Fig. 3. Refined sample LaMg$_2$Ni$_5$Al$_4$-Bin-20h (from binary compounds) using Rietveld method.

Table 1. Lattice parameters and weight fraction of existing phases in LaMg$_2$Ni$_5$Al$_4$-ES-20h sample

Milling time	Phase	Space group	Lattice parameters (Å)	V (Å^3)	Weight fraction (%)	R$_f$	R$_{Bragg}$	χ^2
20h	AB$_3$	R-3m	a = 4.7605(8) c = 24.801(8)	486.76	96	1.0	1.8	1.7
	La$_2$O$_3$	P6$_3$/mmc	a = 3.867(3) c = 5.893(9)	76.34	4	1.1	2.7	

Table 2. Lattice parameters and weight fraction of existing phases in LaMg$_2$Ni$_5$Al$_4$-Bin-20h sample

Milling time	Phase	Space group	Lattice parameters (Å)	V (Å^3)	Weight fraction (%)	R$_f$	R$_{Bragg}$	χ^2
20h	AB$_3$	R-3m	a = 4.7593(7) c = 24.840(7)	487.27	96	1.0	1.8	1.8
	La$_2$O$_3$	P6$_3$/mmc	a = 3.874(3) c = 5.881(9)	76.47	4	1.2	2.8	
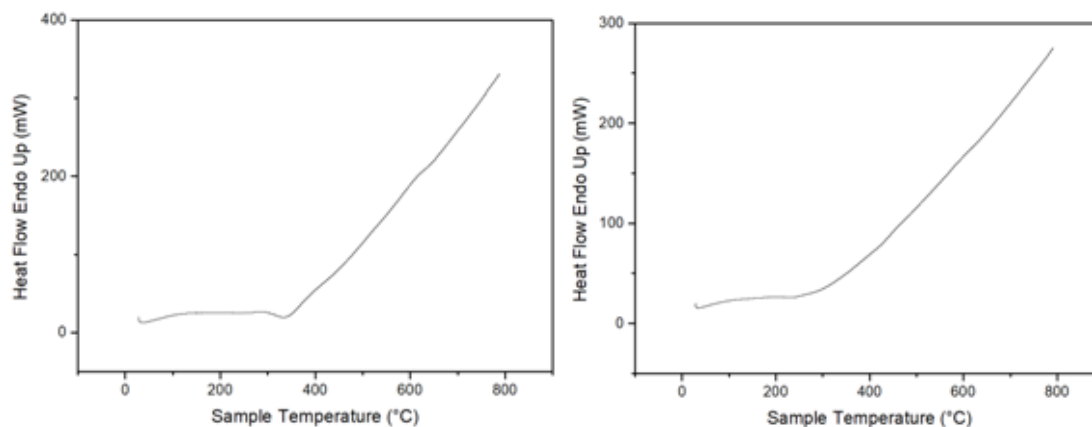
Fig. 4. Differential Thermal analysis DTA of the two AB$_3$ sample

LaMg$_2$Ni$_5$Al$_4$-ES-20h (Left) LaMg$_2$Ni$_5$Al$_4$-Bin-20h (right).

3.1. Differential Thermal Analysis DTA

DTA experiments of the two elaborated AB_3 samples are illustrated on Figure 4. Both DTA curves show an overall uniform variation trend at low and high temperature (300-800 °C) that most likely translate a smooth or minor adjustment related to a very gentle annealing of the mechanically alloyed material and its structure defects recovery. Thermal analysis is very important technique to characterize interstitial AB_x intermetallic compounds and other complex metallic systems especially their temperature of phase transformation or the limit of their manipulation conditions [31-33]. A DTA study on La-Mg-Ni super lattice alloys was reviewed recently by Liu et al. [34], showing a very similar thermal profile to these experiments given in Figures 4. Direct comparison regarding thermal stability of classic AB_5 compound ($LaNi_5$) reveals that the presented AB_3 alloys in this study are substantially more stable and can support higher heating flow [35,36].

3.2. Hydrogen storage evolution

Before the discovery of AB_3 type compounds, the AB_5 ones were the first generation of commercially used alloys and their first patents using $LaNi_{5-x}M_x$ substituted compounds in electrochemical applications (for electrode material) dates from the 1970s [37]. $LaNi_5$ is the best-known compound in AB_5 family with Ni-MH power delivery around 370 mAh/g [38]. In recent progress, AB_3 type compounds are actually the most studied with more interests in terms of absorption-desorption properties for hydrogen storage [39]: their corresponding hydrides are promising to be very efficient for hydrogen loading in stationary or mobile applications or devices [40,41]. These compounds can give energy conversion up to 600 mAh/g when associated with systems of hydrogen compressor [42]. Direct solid-gas processing for the hydrogenation reaction is given in the following Equation:

$$LaMg_2Ni_5Al_4 + x/2\ H_2 \xrightarrow{\substack{P = 10\ bars,\ 230\text{-}280\ °C}} LaMg_2Ni_5Al_4H_x$$
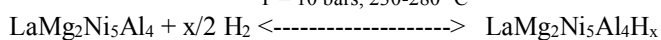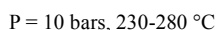
The resulting plot of this experiment for the first sample ($LaMg_2Ni_5Al_4$-ES-20h) is given in Figure 5. It is obviously displayed that hydrogen reaction speed decreases when setting an inferior temperature regarding the curve evolution.
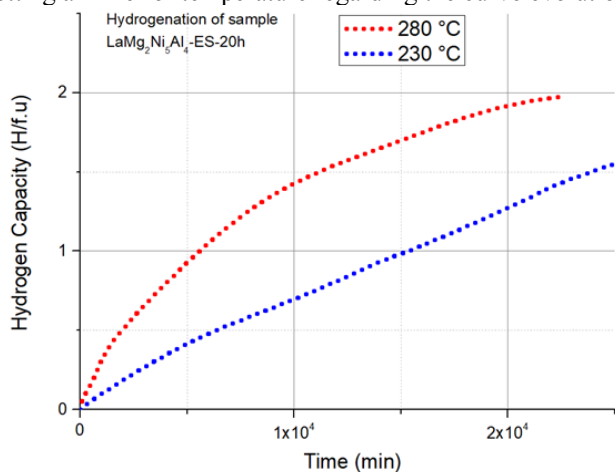

Fig. 5. Variation of hydrogen absorption capacity as function of Time for $LaMg_2Ni_5Al_4$-ES-20h sample.

Several analytical simulation models were developed in literature for the hydrogen storage evolution. Lamloumi et al. [12] proposed a third order equation taking into account both the reaction kinetic k and the equilibrium pressure P_{eq}.

$$\frac{H/M}{(H/M)_{ss}} = 1 - \left[1 - k \cdot t \frac{P(t) - P_{eq}}{P_0 - P_{eq}} P_0^2 \cdot \exp\left(\frac{19,500}{R_gT}\right) \cdot 10^{-6} \right]^3$$

Another more simplified model was later elaborated by Johnson-Mehl [13], where the model considers diffusion and nucleation growth as the controlling rate mechanism with following expression: $f(t) = 1 - exp(-k \cdot t^n)$

Generalized formulation was adopted recently from Avrami-Erofeev [14], that assume the absorption contribution of one or more species depending on the fractions and if any multistep mechanism will be existing:

$$N = A_1\{1 - exp[-(k_1t)^{n_1}]\} + A_2\{1 - exp[-(k_2t)^{n_2}]\}$$

According the major AB_3 phase found in XRD study, it is assessed to correlate overall hydrogenation speed k (min^{-1}) for the obtained data within first-order Avrami exponential fitting for the hydrogen capacity: $C_t = C_{max} exp(-k \cdot t)$ with C_t the real-time capacity, C_{max} the maximum capacity, k the reaction speed and t the time. The coefficient k depends on the temperature conforming to the Arrhenius Law with the formulated following equation [12-14]:

$$k = A \cdot exp(-E/R \cdot T)$$

where A pre-exponential factor, R universal gas constant and E activation energy for the hydrogenation reaction.

Processing of experimental datasets fitting in Figure 6 and 7 determines the values of kinetics parameters respectively $k_{280} = (1.20 \pm 0.08)\ 10^{-4}\ min^{-1}$ and $k_{230} = (1.66 \pm 0.04)\ 10^{-5}\ min^{-1}$.

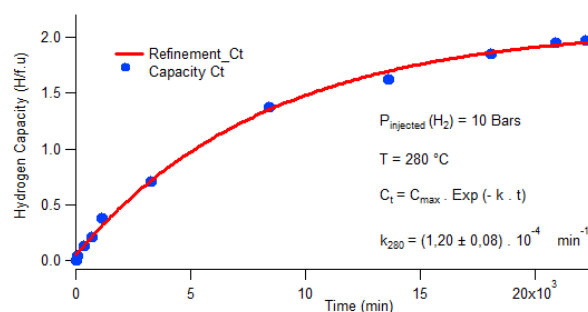**Fig. 6.** Exponential fitting of C_t vs. Time to obtain k_{280} for $LaMg_2Ni_5Al_4$-ES-20h.
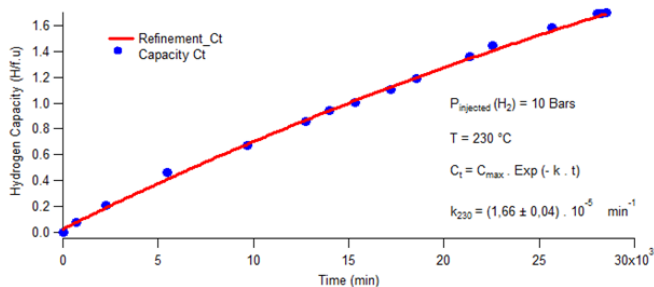
Fig. 7. Exponential fitting of C_t vs. Time to obtain k_{230} for LaMg$_2$Ni$_5$Al$_4$-ES-20h.

We confirm here according to these kinetics refinements that the hydrogen reaction speed is slowing down by 10 folds when the temperature evolves from 280 °C to 230 °C.

The reported temperature dependent hydrogenation kinetics are used to generate the linear graphic plot (Figure 8) through thermodynamic equation [43-45]: **_Ln (k) = Ln (A) - E / R . T_**

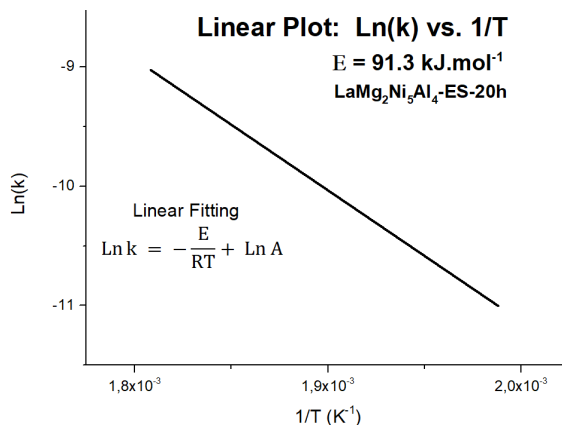**Fig. 8.** Linear fitting of the Ln (k) plot for hydrogenated LaMg$_2$Ni$_5$Al$_4$-ES-20h.

From this plot analysis and slope calculation, we obtained the intermetallic-hydride activation energy for the first sample LaMg$_2$Ni$_5$Al$_4$-ES-20h, E = 91.3 kJ.mol^{-1}.

Same experimental procedure was carried out (Figure 9) for the second sample elaborated by mechanical alloying from binary precursors. This approach will give and setup very interesting comparison between two hydrogenated samples synthesized by two different pathways.
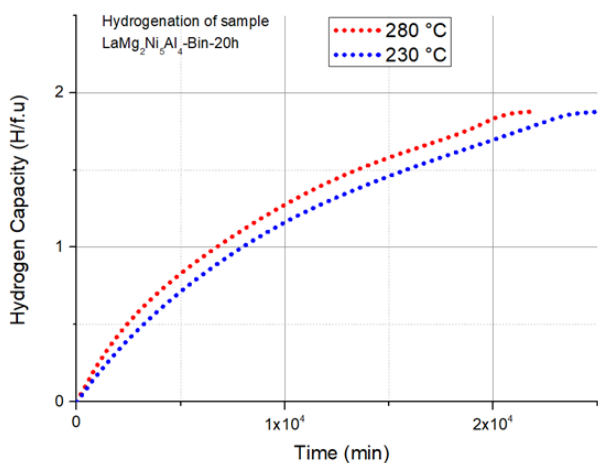

Fig. 9. Variation of hydrogen absorption capacity as function of Time for LaMg$_2$Ni$_5$Al$_4$-Bin-20h sample.

It is noted in this case that when decreasing the temperature, the kinetic curve seems to have a slight shift indicating very slow impact on the hydrogenation speed. Attempt to undergo the same interpolation procedure realized in the previous compound, and the following Figures 10 and 11 are showing the corresponding exponential fitting of the experimental point by point selections for real time hydrogen capacity. According to the obtained mathematical processing, the following values of kinetics parameters are found: respectively k_{280} = (1.06 ± 0.08) 10^{-4} min^{-1} and k_{230} = (9.72 ± 0.02) 10^{-5} min^{-1}.
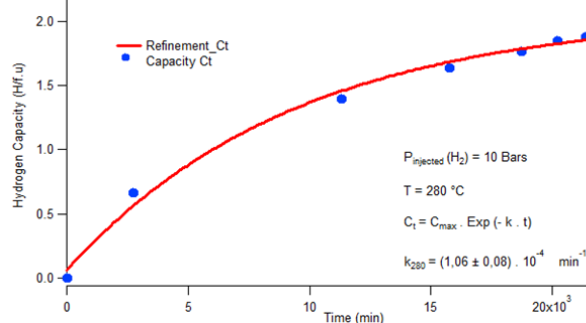

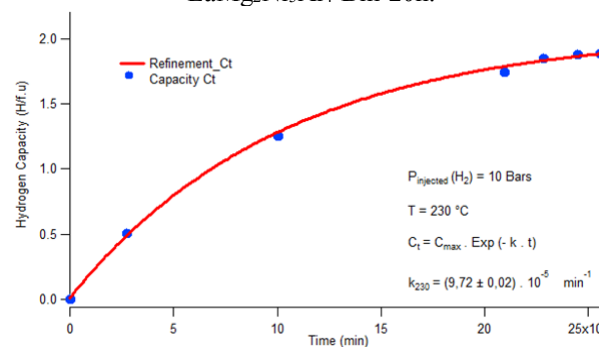**Fig. 10.** Exponential fitting of C_t vs. Time to obtain k_{280} for LaMg$_2$Ni$_5$Al$_4$-Bin-20h.

Fig. 11. Exponential fitting of C_t vs. Time to obtain k_{230} for LaMg$_2$Ni$_5$Al$_4$-Bin-20h.

Finally, the corresponding linear plot was traced for this AB$_3$ compound obtained from the two binary precursors as given in the Figure 12. The calculated hydride activation energy for this second sample LaMg$_2$Ni$_5$Al$_4$-Bin-20h, obtained from the slope of Figure 12, was E = 4.1 kJ.mol^{-1}.
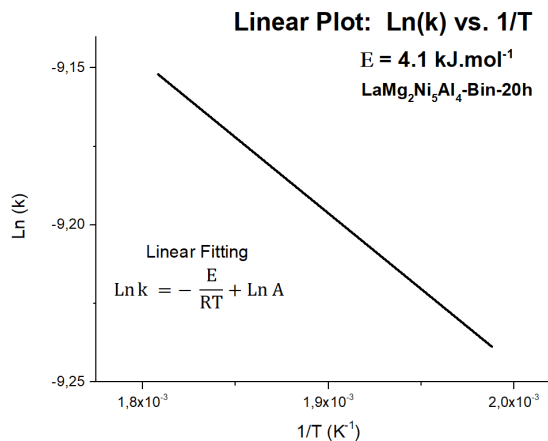
Fig. 12. Linear fitting of the Ln (k) plot for hydrogenated LaMg$_2$Ni$_5$Al$_4$-Bin-20h.

Interestingly from the hydrogenation process in this study, a direct comparison of these results demonstrates and gives clear evidence that AB$_3$ compound obtained from binary precursors undergoes lower activation energy barrier to achieve its hydride regarding the AB$_3$ alloy acquired from pure elements.

Most studies have been done previously on thermodynamic enthalpy formation of AB$_3$H$_x$ and Magnesium based hydrogen storage alloys [15,46,47]. However, we did not find in literature many articles dealing with comparative study of activation energy corresponding to a quaternary Metal-Hydride developed from two different pathways approaches. It was reported that activation energies E$_a$ (examples of simple Magnesium or Titanium hydrides) can reach values up to 120 kJ.mol^{-1} at 10 bars H$_2$ injected pressure depending on temperature or substituting element if applicable [48,49]. Moreover, incorporation of Nickel inside the matrix material seems to drastically decrease E$_a$ by more than 70 kJ.mol^{-1} : which is comparable to an operating catalyzing effect [50]. We are not surprised to find out such lower activation values since other published simple compounds like ZrTiV or TiN$_x$ undergoes E$_a$ values about 5 to 10 kJ.mol^{-1} [51,52]. Another more plausible physical explanation is that AB$_3$ intermetallic compounds elaborated from the binary precursor LaNi$_5$ are usually expected to have more facility to activate the H-H hydrogen-hydrogen bonds (since LaNi$_5$ is known to have high hydrogen affinity especially within direct H$_2$ solid-gas reaction). We note for instance that others AB$_3$ intermetallics are existing in literature with different compositions showing some flexibility in metal substitution possibilities, most likely Aluminum substitution by Nickel seems to stabilize the hydrogen equilibrium pressure however lower hydrogen capacity will be expected [46].

4. Conclusion

This study involves an interesting thermal behavior of a recently developed AB$_3$ compound LaMg$_2$Ni$_5$Al$_4$. Using this alloy and according the thermal DTA analysis, operation temperatures up to 800 °C can be reached with very good stability offering an extra hands-on others possible high temperature applications.

XRD analysis demonstrates that the target crystalline phase is easily obtained using the mechanical alloying procedure with an injected shock power of 12 W/g and using two different synthesis approach.

Two different operation temperatures are used to evaluate kinetics of hydrogenation speed and then the thermodynamic calculation of activation energy.
Successful exponential interpolation of the reaction speed was carried out using Avrami model. Obviously and according the absorption behavior of AB$_3$ intermetallic from binary percursors, it undergoes lower activation energy regarding the parent intermetallic material from elementary metals. This comprative case study conducted in this work shows that the elaborated compounds can be further used in high temperature energy conversion or storage reaction.

These direct solid-gas reactions on substituted Magnesium AB$_3$ alloys can promote and stabilize bulk intermetallic hydrides.

References

[1] W. McDowall, "Exploring possible transition pathways for hydrogen energy: A hybrid approach using socio-technical scenarios and energy system modeling", Futures, vol. 63, pp. 1-14, 2014.

[2] E. Rivard, M. Trudeau, K. Zaghib, "Hydrogen Storage for Mobility: A Review", Materials, vol. 12(2), No. 1973, 2019.

[3] D.P. Broom, C.J. Webb, K.E. Hurst, "Outlook and challenges for hydrogen storage in nanoporous materials", Appl. Phys. A, vol. 122, No. 151, 2016.

[4] K.T. Møller, T.R Jensen, E. Akiba, H-w. Li, "Hydrogen - A sustainable energy carrier", Pro. Nat. Sci-Mater., vol. 27(1), pp. 34-40, 2017.

[5] JB. von Colbe, J-R Ares, J. Barale, M. Baricco, C. Buckley, G. Capurso, N. Gallandat, D.M. Grant, M.N. Guzik, I. Jacob, E.H. Jensen, T. Jensen, J. Jepsen, T. Klassen, M.V. Lototskyy, K. Manickam, A. Montone, J. Puszkiel, S. Sartori, D.A. Sheppard, A. Stuart, G. Walker, C.J. Webb, H. Yang, V. Yartys, A. Züttel, M. Dornheim, "Application of hydrides in hydrogen storage and compression: Achievements, outlook and perspectives", Int. J. Hydrogen Energy, vol. 44(15), pp. 7780-7808, 2019.

[6] J. Abe, A. Popoola, E. Ajenifuja, O.M. Popoola, "Hydrogen energy, economy and storage: Review and recommendation", Int. J. Hydrogen Energy, vol. 44(29), pp. 15072-15086, 2019.

[7] R. Moradi, K.M. Growth, "Hydrogen storage and delivery: Review of the state of the art technologies and risk and reliability analysis", Int. J. Hydrogen Energy, vol. 44(23), pp. 12254-12269, 2019.

[8] J. Chen, H.T. Takeshita, H. Tanaka, N. Kuriyama, T. Sakai, I. Uehara, M. Haruta, "Hydriding properties of LaNi$_3$ and CaNi$_3$ and their substitutes with PuNi$_3$-type structure", J. Alloy. Compd., vol. 302(1-2), pp. 304-313, 2000.

[9] M. Jurczyk, Handbook of Nanomaterials for Hydrogen Storage, Singapore: Pan Stanford, 2017.

[10] W. Liu, C.J. Webb, E.M.A. Gray, "Review of hydrogen storage in AB$_3$ alloys targeting stationary fuel

cell applications", Int. J. Hydrogen Energy, vol. 41(5), pp. 3485-3507, 2016.

[11] B. Liao, Y.Q. Lei, L.X. Chen, G.L. Lu, H.G. Pan, Q.D. Wang, "A study on the structure and electrochemical properties of $La_2Mg(Ni_{0.95}M_{0.05})_9$ (M = Co, Mn, Fe, Al, Cu, Sn) hydrogen storage electrode alloys", J. Alloy. Compd., vol. 379(1-2), pp. 186-195, 2004.

[12] A. Jemni, S. Ben Nasrallah, J. Lamloumi, "Experimental and theoretical study of a metal-hydrogen reactor", Int. J. Hydrogen Energy, vol. 14(7), pp. 631-644, 1999.

[13] R. Sarhaddi, H. Arabi, F. Pourarian, "Structural, morphological, magnetic and hydrogen absorption properties of $LaNi_5$ alloy: A comprehensive study", Int. J. Mod. Phys. B, vol. 28(14), No. 1450079, 2014.

[14] M. Lotoskyy, R. Denys, V.A. Yartys, J. Eriksen, J. Goh, S.N. Nyamsi, C. Sita, F. Cummings, "An outstanding effect of graphite in nano-MgH_2-TiH_2 on hydrogen storage performance", J. Mater. Chem. A, vol. 6, pp. 10740-10754, 2018.

[15] V.B. Son, B.P. Tarasov, "Hydrogen-Sorption Properties of $La_{3-x}Mg_xCo_9$ (x = 1.2, 1.5, and 2) Intermetallic Compounds", Russ. J. Inorg. Chem., vol. 65(2), pp. 147-153, 2020.

[16] H. Jaafar, A. Dhiab, C. Slama, I. Sahli, M. Abdellaoui, "Synthesis of quaternary nano-intermetallic $LaTi_2Ni_5Al_4$ with its hydrogen encapsulation and inspection using lithium-hydride cell", Micro Nano Lett., vol. 15(3), pp. 201-205, 2020.

[17] Q. Luo, J. Li, B. Li, B. Liu, H. Shao, Q. Li, "Kinetics in Mg-based hydrogen storage materials: Enhancement and mechanism", J. Magnes. Alloy., vol. 7(1), pp. 58-71, 2019.

[18] Y. Zhang, P. Wang, W. Bu, Z. Yuan, Y. Qi, S. Guo, "Improved hydrogen storage kinetics of nanocrystalline and amorphous Ce-Mg-Ni-based $CeMg_{12}$-type alloys synthesized by mechanical milling", RSC Adv., vol. 8, pp. 23353-23363, 2018.

[19] Y. Sun, C. Shen, Q. Lai, W. Liu, D-W. Wang, K-F Aguey-Zinsou, "Tailoring magnesium based materials for hydrogen storage through synthesis: Current state of the art", Energy Storage Mater., vol. 10, pp. 168-198, 2018.

[20] W. Wang, W. Guo, X. Liu, S. Zhang, Y. Zhao, Y. Li, L. Zhang, S. Han, "The interaction of subunits inside superlattice structure and its impact on the cycling stability of AB_4-type La-Mg-Ni-based hydrogen storage alloys for nickel-metal hydride batteries", J. Power Sources, vol. 445, No. 227273, 2020.

[21] X. Zhao, D. Ke, Y. Cai, F. Hu, Dr. J. Liu, L. Zhang, S. Han, "A Novel Synthesis Method of La-Mg-Ni-based Superlattice by $LaNi_5$ Absorbing Gas-state Mg", ChemistrySelect, vol. 4(27), pp. 8165-8170, 2019.

[22] W. Wang, R. Qin, R. Wu, X. Tao, H. Zhang, Z. Ding, Y. Fu, L. Zhang, L. Wu, Y. Li, S. Han, "A promising anode candidate for rechargeable nickel metal hydride power battery: An A_5B_{19}-type La-Sm-Nd-Mg-Ni-Al-based hydrogen storage alloy", J. Power Sources, vol. 465, No. 228236, 2020.

[23] Y. Zhang, H. Sun, W. Zhang, Z. Yuan, X. Wei, J. Gao, H. Ren, "Improvement of substituting La with Ce on hydrogen storage thermodynamics and kinetics of Mg-based alloys", Int. J. Hydrogen Energy, vol. 46(56), pp. 28719-28733, 2021.

[24] E.M. Dematteis, N. Berti, F. Cuevas, M. Latroche, M. Baricco, "Substitutional effects in TiFe for hydrogen storage: a comprehensive review", Mater. Adv., vol. 2, pp. 2524-2560, 2021.

[25] M. Shatnawi, N. Al Qaydi, N. Aljaberi, M. Aljaberi, "Hydrogen-Based Energy Storage Systems: A Review", 7th International Conference on Renewable Energy Research and Applications (ICRERA), pp. 697-700, 14-17 October 2018.

[26] Y. Takmi, Y. Takaki, M. Shinohara, Y. Matsuda, H. Fujiyama, "Hydrogenation of Si(110) surface due to hydrogen plasma exposure, investigated with in-situ MIR-IRAS", International Conference on Renewable Energy Research and Applications (ICRERA), pp. 1-3, 11-14 November 2012.

[27] B. Zafar, "Design of a Renewable hybrid photovoltaic-Electrolyze-PEM/Fuel Cell System using Hydrogen Gas", International Journal of Smart Grid, vol. 3, No. 4, pp. 201-207, 2019.

[28] S. Gherairi, "Zero-Emission Hybrid Electric System: Estimated Speed to Prioritize Energy Demand for Transport Applications", International Journal of Smart Grid, vol. 3, No. 4, pp. 180-187, 2019.

[29] J. Morel, S. Obara, K. Sato, D. Mikawa, H. Watanabe and T. Tanaka, "Contribution of a hydrogen storage-transportation system to the frequency regulation of a microgrid", International Conference on Renewable Energy Research and Applications (ICRERA), pp. 510-514, 22-25 November 2015.

[30] H. Jaafar, L. Aymard, W. Dachraoui, A. Demortière, M. Abdellaoui, "Preparation and characterization of mechanically alloyed AB_3-type based material $LaMg_2Ni_5Al_4$ and its solid-gaz hydrogen storage reaction", J. Solid State Chem., vol. 260, pp. 73-79, 2018.

[31] D.P. Broom, Hydrogen Storage Materials: The Characterisation of Their Storage Properties, Green Energy and Technology, London: Springer-Verlag, 2011.

[32] G. Walker, Solid-State Hydrogen Storage: Materials and Chemistry, Cambridge England: 1st Edition Woodhead Publishing, 2008.

[33] S.A. Sherif, D.Y. Goswami, E.K. Stefanakos, A. Steinfeld, Handbook of Hydrogen Energy 1st Edition, Florida USA: CRC Press Taylor & Francis, 2014.

[34] J. Liu, S. Han, Y. Li, L. Zhang, Y. Zhao, S. Yang, B. Liu, "Phase structures and electrochemical properties of La-Mg-Ni-based hydrogen storage alloys with

superlattice structure", Int. J. Hydrogen Energy, vol. 41(44), pp. 20261-20275, 2016.

[35] J. Kleperis, L. Grinberga, M. Ergle, G. Chikvaidze, J. Klavins, "Thermogravimetric research of hydrogen storage materials", J. Phys.: Conf. Ser., vol. 93, No. 012027, 2007.

[36] M.V. Blanco, E. Zelaya, M.R. Esquivel, "Study of the Thermal Stability in Air of $LaNi_5$ by DSC, EDX, TEM and XRD Combined Techniques", Procedia Mater. Sci., vol. 1, pp. 564-571, 2012.

[37] F. Cuevas, J-M. Joubert, M. Latroche, A. Percheron-Guégan, "Intermetallic compounds as negative electrodes of Ni/MH batteries", Appl. Phys. A, vol. 72(2), pp. 225-238, 2001.

[38] K. Buschow, H. Van Mal, A. Miedema, "Hydrogen absorption in intermetallic compounds of thorium", J. Less Common Met., vol. 42(2), 163-178, 1975.

[39] G. Sandrock, "A panoramic overview of hydrogen storage alloys from a gas reaction point of view", J. Alloy. Compd., vol. 293-295, pp. 887-888, 1999.

[40] M. Hirscher, V.A. Yartys, M. Baricco, JB.von Colbe, D. Blanchard, R.C. Bowman, D.P. Broom, C.E. Buckley, F. Chang, P. Chen, Y. Whan Cho, J-C Crivello, F. Cuevas, W.I.F. David, P.E. de Jongh, R.V. Denys, M. Dornheim, M. Felderhoff, C Zlotea, "Materials for hydrogen-based energy storage - past, recent progress and future outlook", J. Alloy. Compd., vol. 827, No. 153548, 2020.

[41] K. Manickam, P. Mistry, G. Walker, D. Grant, C.E. Buckley, T.D. Humphries, M. Paskevicius, T. Jensen, R. Albert, K. Peinecke, M. Felderhoff, "Future perspectives of thermal energy storage with metal hydrides", Int. J. Hydrogen Energy, vol. 44(15), pp. 7738-7745, 2019.

[42] K. Kadir, T. Sakai, I. Uehara, "Structural investigation and hydrogen capacity of YMg_2Ni_9 and $(Y_{0.5}Ca_{0.5})(MgCa)Ni_9$: new phases in the AB_2C_9 system isostructural with $LaMg_2Ni_9$", J. Alloy. Compd., vol. 287(1-2), pp. 264-270, 1999.

[43] A. Andreasen, "Hydrogenation properties of Mg-Al alloys", Int. J. Hydrogen Energy, vol. 33(24), pp. 7489-7497, 2008.

[44] M. Zhu, Y. Lu, L. Ouyang, H. Wang, "Thermodynamic Tuning of Mg-Based Hydrogen Storage Alloys: A Review", Materials, vol. 6(10), pp. 4654-4674, 2013.

[45] A. Züttel, "Hydrogen storage methods", Naturwissenschaften, vol. 91(4), pp. 157-172, 2004.

[46] M. Latroche, in: E. Burzo (Eds.), Hydrogen Storage Materials, Advanced Materials and Technologies, Berlin: Springer, 2018, vol. 8, pp. 151-157.

[47] A. Baran, M. Polański, "Magnesium-Based Materials for Hydrogen Storage-A Scope Review", Materials, vol. 13(18), No. 3993, 2020.

[48] A. Perejón, P.E. Sánchez-Jiménez, J.M. Criado, "Magnesium hydride for energy storage applications: The kinetics of dehydrogenation under different working conditions", J. Alloy. Compd., vol. 681, pp. 571-579, 2016.

[49] P.M. Grigoreva, Y.A. Yakovlev, A.M. Polyanskiy, in: V.A. Polyanskiy, A.K. Belyaev (Eds.), Advances in Hydrogen Embrittlement Study, Advanced Structured Materials, Switzerland: Springer, 2021, vol. 143, pp. 131-142.

[50] X. Yang, Q. Hou, L. Yu, J. Zhang, "Improvement of the hydrogen storage characteristics of MgH_2 with a flake Ni nano-catalyst composite", Dalton Trans., vol. 50, pp. 1797-1807, 2021.

[51] Y. Zhang, J. Li, T. Zhang, T. Wu, H. Kou, X. Xue, "Hydrogenation thermokinetics and activation behavior of non-stoichiometric Zr-based Laves alloys with enhanced hydrogen storage capacity", J. Alloy. Compd., vol. 694, pp. 300-308, 2017.

[52] C. Kura, Y. Kunisada, E. Tsuji, C. Zhu, H. Habazaki, S. Nagata, M.P. Müller, R.A. De Souza, Y. Aoki, "Hydrogen separation by nanocrystalline titanium nitride membranes with high hydride ion conductivity", Nat. Energy, vol. 2, pp. 786-794, 2017.